JACS
JOURNAL OF THE AMERICAN CHEMICAL SOCIETY
Communication
pubs.acs.org/JACS

Synthesis and Properties of Two Cationic Narrow Band Gap Conjugated Polyelectrolytes

Zachary B. Henson,[†] Yuan Zhang,[†] Thuc-Quyen Nguyen,[†] Jung Hwa Seo,*[,‡] and Guillermo C. Bazan*[,†]

[†]Center for Polymers and Organic Solids, Department of Chemistry & Biochemistry, Department of Materials, University of California, Santa Barbara, California 93106, United States

[‡]Department of Materials Physics, College of Natural Science, Dong-A University, Busan, 604-714, South Korea

Supporting Information

ABSTRACT: We report the design, synthesis, and optical and electronic properties of two novel narrow band gap conjugated polyelectrolytes (NBGCPEs) based on a poly[2,6-(4,4-bis-alkyl-4*H*-cyclopenta[2,1-*b*;3,4-*b*′]dithiophene)-*alt*-4,7-(2,1,3-benzothiadiazole)] donor/acceptor backbone. Comparison with the properties of the neutral precursor material shows that the ionic component in these cationic NBGCPEs leads to a red-shift in the absorption spectra and to a modification of the polymer electronic energy levels. Both the HOMO and the LUMO are lowered in energy, with the net effect being dependent on the choice of counterion, i.e. bromide vs tetrakis(1-imidazolyl)borate. Moreover, we unexpectedly find n-type transport in thin-film transistors, as opposed to the widely studied p-type transport in neutral systems with isoelectronic backbones. From these observations we conclude that introduction of ionic functionalities adjacent to semiconducting polymers that exhibit charge-transfer excitations offers unique opportunities for materials design.

Narrow band gap conjugated polymers (NBGCPs) and conjugated polyelectrolytes (CPEs) are two broad classes of polymeric semiconductors under investigation because of their relevance to various emerging optoelectronic technologies.[1] NBGCPs have shown promise as functional materials because their optical properties can be fine-tuned to match the solar spectrum and because their orbital energy levels can be adjusted to favor photoinduced charge transfer (CT) to other semiconductors and charge injection into or extraction from metal electrodes.[1d,2] NBGCPs are therefore excellent materials for the fabrication of bulk heterojunction organic solar cells[1,3] and n-type,[4] p-type,[5] or ambipolar[6] field-effect transistors.

CPEs are defined by a π-delocalized backbone with pendant ionic functionalities.[7] They combine the light-harvesting and charge transport capabilities of conjugated polymers with the physical characteristics of polyelectrolytes, which can be mediated by electrostatic interactions.[8] Their polar nature provides the opportunity for more environmentally friendly processing conditions and facile methods for generating multilayer device structures. CPEs have been recently employed as electron injection/transport layers between neutral organic semiconducting layers and metal electrodes to improve charge injection in organic light-emitting diodes (OLEDs)[9] and organic field-effect transistors (OFETs)[10] and charge extraction in organic photovoltaic devices (OPVs).[11] Additionally, they can be used as sensitizers in dye-sensitized solar cells.[12]

Literature reports point to the ionic component in CPEs being able to modulate relevant optoelectronic properties. For example, changing the size of the charge-compensating ions can decrease interchain contacts and thereby emission quantum yields and charge carrier mobilities.[13] CT state stabilization has also been observed in a CPE copolymer.[14] Exciton binding energies are also changed compared to those of the neutral analogues.[15] Although detailed structure/property relationships are not yet available, these observations indicate a substantial influence by the ionic component on properties relevant to devices. However, the physical and electronic properties of narrow band gap CPEs (NBGCPEs) remain largely unexplored. To begin addressing this area of scientific inquiry, we report herein the synthesis of cationic NBGCPEs with a backbone containing alternating donor/acceptor units that lead to CT excitons, and examine the effect of the ionic component on the optical and electronic properties. Unexpectedly, we find that, unlike the neutral precursor counterpart, cationic NBGCPE with an appropriate counterion exhibits n-type behavior within a thin-film transistor configuration.

Our choice for building a cationic NBGCPE takes advantage of the poly[2,6-(4,4-bis-alkyl-4*H*-cyclopenta-[2,1-*b*;3,4-*b*′]-dithiophene)-*alt*-4,7-(2,1,3-benzothiadiazole)] framework. Scheme 1 shows the molecular structures and the synthetic entry. Detailed synthetic procedures can be found in the Supporting Information (SI). Briefly, Suzuki cross-coupling polymerization of an alkyl bromide-substituted cyclopentadithiophene and the bis-boronic ester of benzothiadiazole was used to generate the neutral precursor polymer, **PCPDTBT-Br**. Post-polymerization quaternization with pyridine introduced the cationic functionalities and yielded **PCPDTBT-Pyr$^+$Br$^-$**. As a final chemical modification, the bromide counterions in **PCPDTBT-Pyr$^+$Br$^-$** were exchanged with the larger tetrakis(1-imidazolyl)borate (BIm_4^-) anion to provide **PCPDTBT-Pyr$^+$BIm$_4^-$**. The choice of BIm_4^- counterion was based on previous results incorporating CPEs as electron injection layers in OLEDs and OFETs.[7c,10,16] Ion exchange was verified by X-ray photoelectron spectroscopy (XPS) and NMR spectroscopy (see SI). The number-average molecular weight of **PCPDTBT-Br** was determined by gel permeation chromatography at 150 °C in 1,2,4-trichlorobenzene to be ~5 kg/mol. This low molecular weight is due to poor

Received: July 25, 2012
Published: March 5, 2013

   dx.doi.org/10.1021/ja400140d | *J. Am. Chem. Soc.* 2013, 135, 4163−4166

Scheme 1. Synthesis of the NBGCP Precursor PCPDTBT-Br and Conversion to Polyelectrolytes PCPDTBT-Pyr$^+$Br$^-$ and PCPDTBT-Pyr$^+$BIm$_4^-$ [a]

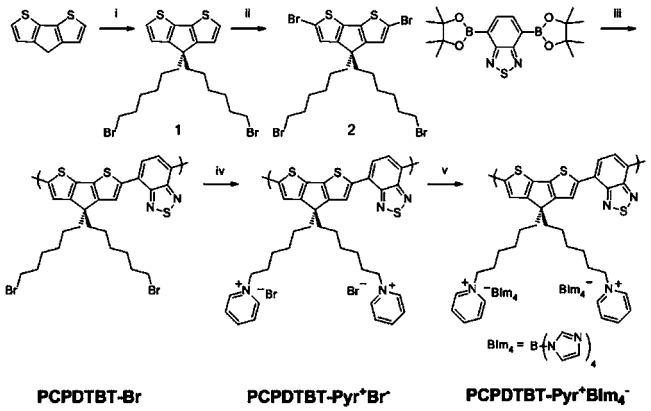

[a](i) KOH, $C_6H_{12}Br_2$, toluene, 80°C, 5h. (ii) NBS, DMF, dark, 20min. (iii) $K_2CO_{3(aq)}$, $Pd(PPh_3)_4$, Bu_4NBr, THF, 85°C, 24h. (iv) Pyridine, 100°C, 48h. (v) Sodium tetrakis(1-imidazolyl)borate, MeOH.

solubility of **PCPDTBT-Br** in the reaction mixture, most reasonably a result of insufficient alkyl chain bulk.[17] Indeed, higher molecular weight can be achieved by incorporating longer alkyl bromide (e.g., octyl bromide) side chains; however, the resulting polyelectrolyte species are then rendered less soluble due to their amphiphilic nature. A balance must therefore be found between the size and nature of the side chain so that both the neutral precursor and charged polyelectrolyte product are soluble for processing into thin-film devices. The number of repeat units of both NBGCPEs was assumed to be unchanged from the neutral precursor by the quaternization and ion-exchange reactions. Thermal transitions were not detected for any of the polymers as measured by differential scanning calorimetry between 0 and 300 °C.

Figure 1a gives solution and solid-state absorption spectra of **PCPDTBT-Br**, **PCPDTBT-Pyr$^+$Br$^-$**, and **PCPDTBT-Pyr$^+$-BIm$_4^-$**. Polymer solutions and films were prepared using chlorobenzene for **PCPDTBT-Br** and methanol for **PCPDT-BT-Pyr$^+$Br$^-$** and **PCPDTBT-Pyr$^+$BIm$_4^-$**. The two cationic polyelectrolytes exhibit similar absorption spectra in solution, showing maximum absorption (λ_{max}) at 705 nm and onset of absorption (λ_{onset}) at 865 nm, which are red-shifted relative to those of the **PCPDTBT-Br** precursor (672 and 785 nm, respectively). All polymers exhibit red-shifted absorption in the solid state compared to solution, and a similar trend is observed with a red-shift in λ_{max} and λ_{onset} for the polyelectrolytes relative to the neutral precursor. While there is no significant difference in λ_{onset} (915 nm) of the polyelectrolytes, λ_{max} of **PCPDTBT-Pyr$^+$BIm$_4^-$** is red-shifted by 18 nm relative to **PCPDTBT-Pyr$^+$Br$^-$**. It is important to note that the red-shift in solution for the charged polymers cannot be broken down into possible contributions from electrostatic perturbation by ions in close proximity to the optically active segment, solvatochromic effects arising from the polar solvent,[3,18] or multichain aggregation.[19] Since no solvent is present, the red-shifted absorption in the film is more reasonably attributed to electrostatic modification of the ground-state electronic structure by the ion's Coulombic field, although possible differences in coil structure and degree of aggregation cannot be ruled out. That **PCPDTBT-Pyr$^+$BIm$_4^-$** exhibits more red-shifted spectra suggests that more intimate

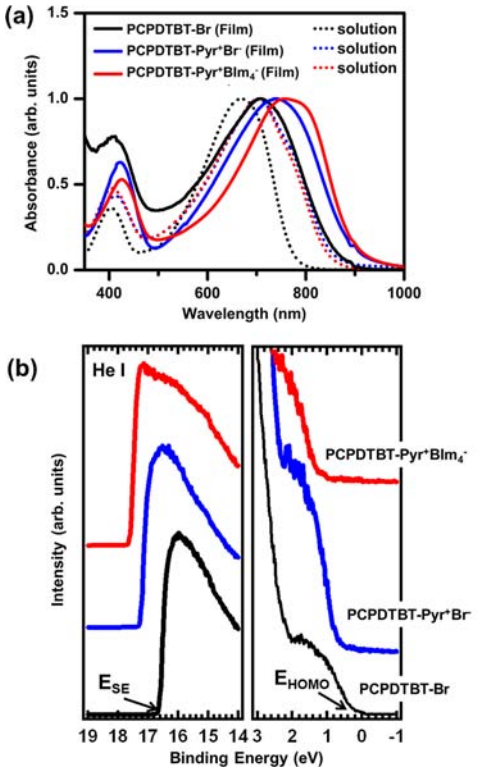

Figure 1. (a) UV–vis absorption spectra of **PCPDTBT-Br** (black), **PCPDTBT-Pyr$^+$Br$^-$** (blue), and **PCPDTBT-Pyr$^+$BIm$_4^-$** (red) solution (dot lines) and films (solid lines) on glass substrates. (b) UPS spectra of three polymer films on Au substrates. The abscissa is the binding energy relative to the Fermi energy of Au (E_{SE}, secondary cutoff energy; E_{HOMO}, HOMO onset energy).

chain contact is not important, as the BIm$_4^-$ ion is larger and more readily separates chains, compared to bromide.[13]

Figure 1b shows the ultraviolet photoelectron spectroscopy (UPS) spectra for films of **PCPDTBT-Br**, **PCPDTBT-Pyr$^+$Br$^-$**, and **PCPDTBT-Pyr$^+$BIm$_4^-$** spin-coated atop Au substrates; the abscissa is the binding energy relative to the Fermi level of Au (E_F), which is defined by the energy of the electron before excitation relative to the vacuum level. The highest occupied molecular orbital onsets (E_{HOMO}) were obtained in the low binding energy region (0–3 eV). This analysis shows that the E_{HOMO} = 0.03 eV for **PCPDTBT-Br**, while E_{HOMO} = 0.75 and 1.31 eV for **PCPDTBT-Pyr$^+$Br$^-$** and **PCPDTBT-Pyr$^+$BIm$_4^-$** films, respectively. In the high binding energy region (14–19 eV), the two cationic polymers exhibit a shift toward higher binding energy relative to the neutral polymer. Such a shift suggests the presence of an interfacial dipole at the polymer/Au interfaces, which is attributed to preferential accumulation of anions adjacent to the metal surface.[20]

Table 1 summarizes the energy levels determined from UPS and optical absorption. The ionization potential (IP) and electron affinity (EA) are therefore shifted to more positive values for the charged **PCPDTBT-Pyr$^+$BIm$_4^-$** (4.91 and 3.53 eV) relative to the neutral **PCPDTBT-Br** (4.49 and 3.05 eV), indicating the polyelectrolyte has a lower tendency to be oxidized and is more easily reduced. Energies for the HOMO and LUMO, also estimated by cyclic voltammetry (CV) of thin films (see SI), reveal no differences in the HOMO energy levels within experimental error whether pendant groups are charged or not. However, the LUMO is slightly modified toward more negative

dx.doi.org/10.1021/ja400140d | J. Am. Chem. Soc. 2013, 135, 4163–4166

Table 1. Summary of Molecular Energy Levels (in eV) Obtained via UPS, UV−Vis Absorption, and CV

polymer	IP[a]	EA[b]	E_g[c]	HOMO[d]	LUMO[d]	E_g[d]
PCPDTBT-Br	4.49	3.05	1.44	−4.7	−3.3	1.4
PCPDTBT-Pyr$^+$Br$^-$	4.70	3.31	1.38	−4.7	−3.4	1.3
PCPDTBT-Pyr$^+$BIm$_4^-$	4.91	3.53	1.38	−4.7	−3.5	1.2

[a]Obtained from UPS measurements. [b]Estimated by using the IP value and the optical E_g. [c]Estimated from the onset of film absorption. [d]Obtained from CV measurements.

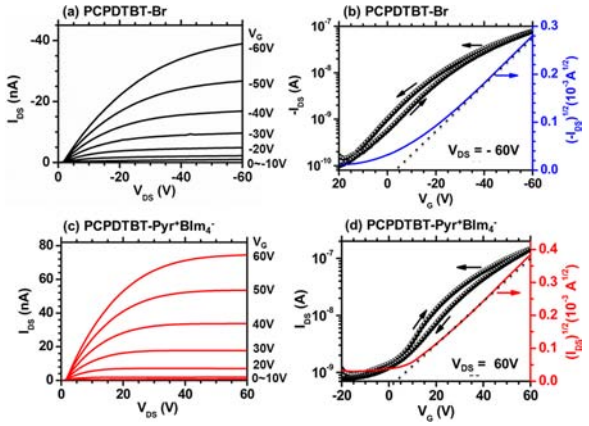

Figure 2. (a) Output and (b) transfer characteristics of a **PCPDTBT-Br** FET under p-type operation at room temperature. (c) Output and (d) transfer characteristics of a **PCPDTBT-Pyr$^+$BIm$_4^-$** FET under n-type operation after annealing at 110 °C.

values (−3.3 eV for **PCPDTBT-Br** vs −3.5 eV for **PCPDTBT-Pyr$^+$BIm$_4^-$**), consistent with the conclusion based on UPS that the NBGCPEs are more easily reduced. Although the CV-determined energy gap (E_g) values are slightly narrower than those determined by optical absorption, one observes a similar trend, with **PCPDTBT-Pyr$^+$BIm$_4^-$** having the smallest gap.

FET hole mobilities as high as 3 cm^2/V·s have been obtained with neutral conjugated polymers that are structurally related to **PCPDTBT-Br**.[1c,5,21] With this in mind, we examined carrier mobilities within a bottom-gate top-contact FET architecture. Polymer layers were deposited by spin-casting from a 0.5% (w/v) chlorobenzene solution for **PCPDTBT-Br** and 0.7% (w/v) methanol solutions for **PCPDTBT-Pyr$^+$Br$^-$** and **PCPDTBT-Pyr$^+$BIm$_4^-$**.

Figure 2 shows the output and transfer characteristics of **PCPDTBT-Br** and **PCPDTBT-Pyr$^+$BIm$_4^-$** FETs. The **PCPDTBT-Br** device showed typical p-type transistor behavior at negative gate bias (V_G = −60 V). In marked contrast, **PCPDTBT-Pyr$^+$BIm$_4^-$** predominately displays n-type transistor behavior under positive bias (V_G = 60 V). Over 20 transistors were measured under a nitrogen atmosphere, all of which confirmed this observation. Note that **PCPDTBT-Pyr$^+$Br$^-$** devices exhibited no FET behavior when either negative or positive V_G was applied. A linear fit was applied in the saturation region of drain/source current $(I_{DS})^{1/2}$ vs V_G curves (Figure 2b,d) to estimate the saturated charge carrier mobilities, according to the saturation current equation, $I_{DS} = (\mu WC/2L)(V_G - V_{th})$.[22] The highest hole mobility for **PCPDTBT-Br** was 6×10^{-5} cm^2/V·s, while an electron mobility as high as −1×10^{-4} cm^2/V·s was obtained for **PCPDTBT-Pyr$^+$BIm$_4^-$**. Table 2 summarizes the performance of devices studied here. Various annealing temperatures for **PCPDTBT-Br** devices

Table 2. FET Device Summary[a]

polymer	μ (cm^2/V·s)[a]	V_{th} (V)[b]	I_{on}/I_{off}[c]
PCPDTBT-Br	6×10^{-5}	−1.6	5×10^2
PCPDTBT-Pyr$^+$BIm$_4^-$	−1×10^{-4}	1.0	2×10^2

[a]Field-effect mobility. [b]Threshold voltage. [c]Current on/off ratio.

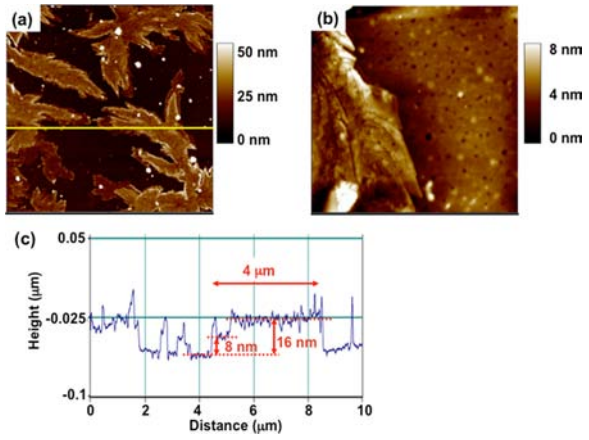

Figure 3. (a) Surface topographic AFM image of **PCPDTBT-Pyr$^+$BIm$_4^-$** on bare SiO_2 surface (10 μm^2). (b) Zoom-in image (2 μm^2) of (a). (c) Surface profile corresponding to (a).

exhibited little effect on the hole mobility. In contrast, the electron mobility of **PCPDTBT-Pyr$^+$BIm$_4^-$** after annealing at 110 °C increased 2-fold compared to the as-cast device. Processing modifications such as gate dielectric passivation and incorporating Al as source and drain electrodes did not improve mobilities (SI). It is also worth noting that a bilayer device in which **PCPDTBT-Pyr$^+$BIm$_4^-$** is deposited atop **PCPDTBT-Br** did not exhibit n-type behavior (Figure S18).

Figure 3a shows the topography of **PCPDTBT-Pyr$^+$BIm$_4^-$** atop a bare SiO_2 surface obtained by atomic force microscopy (AFM), with film casting and substrate conditions identical to those for Figure 2d. Film coverage is not homogeneous; instead, one observes leaf-shaped domains. The 2 μm^2 zoomed-in image in Figure 3b shows a relatively smooth surface (rms 1.6 nm), albeit pinholes are evident. Figure 3c shows the height distribution along the line highlighted in yellow in (a), indicating that in this region the leaf-shaped features exhibit a two-layer structure 8 nm high and 4 μm wide. Thus, the film-forming tendencies of **PCPDTBT-Pyr$^+$BIm$_4^-$** on SiO_2 as cast from methanol are not ideal. It appears that electron transport within the channel in FETs may be taking place along a network of interconnected domains, although the presence of a very thin polymer layer along the dielectric interface cannot be ruled out at this stage. One may anticipate that more continuous films may be obtained for higher molecular weight samples if monomer modification can be carried out to improve the solubility of the precursor material without compromising solubility of the subsequent polyelectrolytes.

To summarize, we have developed a synthetic methodology for accessing cationic polyelectrolytes with NBGCPEs. By comparison against the neutral precursor with the same conjugated framework, one finds that the optical transitions of the NBGCPEs are red-shifted, particularly in the solid state, where the presence of the ions is likely to provide local electrostatic fields that impact intrachain charge-transfer excitations. More significantly, UPS measurements provide evidence that the ionic component also changes the orbital

dx.doi.org/10.1021/ja400140d | J. Am. Chem. Soc. 2013, 135, 4163−4166

energy levels. With **PCPDTBT-Pyr$^+$Br$^-$** and **PCPDTBT-Pyr$^+$BIm$_4^-$** one finds a lowering of the energies for both the LUMO and the HOMO. A more pronounced effect occurs with BIm_4^- relative to Br^-. Our current thinking is that the weaker pyridinium/BIm_4^- ion-pairing leads to a stronger electrostatic effect in proximity to the conjugated backbone. The demonstration that **PCPDTBT-Pyr$^+$BIm$_4^-$** can function as an n-type semiconductor within a FET device was unexpected. One possible scenario is that the ionic functionalities can provide electrostatic dipoles at the electrode that reduce barriers to charge injection; such a mechanism has been widely discussed previously. Indeed, we see that both **PCPDTBT-Pyr$^+$Br$^-$** and **PCPDTBT-Pyr$^+$BIm$_4^-$** are effective interlayers to improve OPV function.[11c,d,23] However, that a thin layer of **PCPDTBT-Pyr$^+$BIm$_4^-$** atop **PCPDTBT-Br** does not yield similar results indicates that interfacial effects alone are insufficient for realizing n-type FET transport. Another possibility is that, as discussed above, lowering the orbital energy levels could stabilize the radical anion (polaron) in ways not readily available for structurally related but neutral conjugated polymers. More work is required to untangle these and other[24] possibilities. Finally, it is worth mentioning that transistor gating behavior is not readily observed with other conjugated polyelectrolytes, as ion migration[25] can redistribute internal fields and complicate the function of the devices. All these observations point out that narrow band gap conjugated polyelectrolytes provide new possibilities to obtain materials with combinations of properties that may find unique applications.

■ ASSOCIATED CONTENT

Ⓢ Supporting Information

Experimental details and characterization data. This material is available free of charge via the Internet at http://pubs.acs.org.

■ AUTHOR INFORMATION

Corresponding Author

seojh@dau.ac.kr; bazan@chem.ucsb.edu

Notes

The authors declare no competing financial interest.

■ ACKNOWLEDGMENTS

The authors are grateful to the National Science Foundation (DMR 1005546, materials design and synthesis), the National Research Foundation of Korea (2011-0030885), and the U.S. Department of Energy, BES (DE-SC0002368, charge injection measurements), for financial support. Z.B.H. thanks the Corning Incorporated Foundation for a fellowship. The MRL Shared Experimental Facilities are supported by the National Science Foundation under award NSF DMR 1121053. We gratefully thank Dr. B. Walker for help with reproducing the FET and AFM results.

■ REFERENCES

(1) (a) Gendron, D.; Leclerc, M. *Energy Environ. Sci.* **2011**, *4*, 1225. (b) Chen, H. Y.; Hou, J. H.; Zhang, S. Q.; Liang, Y. Y.; Yang, G. W.; Yang, Y.; Yu, L. P.; Wu, Y.; Li, G. *Nat. Photon.* **2009**, *3*, 649. (c) Coffin, R. C.; Peet, J.; Rogers, J.; Bazan, G. C. *Nature Chem.* **2009**, *1*, 657. (d) Beaujuge, P. M.; Amb, C. M.; Reynolds, J. R. *Acc. Chem. Res.* **2010**, *43*, 1396. (e) Brabec, C. J.; Gowrisanker, S.; Halls, J. J. M.; Laird, D.; Jia, S.; Williams, S. P. *Adv. Mater.* **2010**, *22*, 3839.

(2) Facchetti, A. *Chem. Mater.* **2010**, *23*, 733.

(3) Cheng, Y. J.; Yang, S. H.; Hsu, C. S. *Chem. Rev.* **2009**, *109*, 5868.

(4) (a) Anthony, J. E.; Facchetti, A.; Heeney, M.; Marder, S. R.; Zhan, X. *Adv. Mater.* **2010**, *22*, 3876. (b) Usta, H.; Facchetti, A.; Marks, T. J. *Acc. Chem. Res.* **2011**, *44*, 501.

(5) Tsao, H. N.; Cho, D. M.; Park, I.; Hansen, M. R.; Mavrinskiy, A.; Yoon, D. Y.; Graf, R.; Pisula, W.; Spiess, H. W.; Müllen, K. *J. Am. Chem. Soc.* **2011**, *133*, 2605.

(6) Ortiz, R. P.; Herrera, H.; Seoane, C.; Segura, J. L.; Facchetti, A.; Marks, T. J. *Chem.—Eur. J.* **2012**, *18*, 532.

(7) (a) Patil, A. O.; Ikenoue, Y.; Wudl, F.; Heeger, A. J. *J. Am. Chem. Soc.* **1987**, *109*, 1858. (b) Huang, F.; Wu, H.; Cao, Y. *Chem. Soc. Rev.* **2010**, *39*, 2500. (c) Hoven, C. V.; Garcia, A.; Bazan, G. C.; Nguyen, T.-Q. *Adv. Mater.* **2008**, *20*, 3793. (d) Jiang, H.; Taranekar, P.; Reynolds, J. R.; Schanze, K. S. *Angew. Chem., Int. Ed.* **2009**, *48*, 4300.

(8) Pace, G.; Tu, G.; Fratini, E.; Massip, S.; Huck, W. T. S.; Baglioni, P.; Friend, R. H. *Adv. Mater.* **2010**, *22*, 2073.

(9) (a) Ma, W.; Iyer, P. K.; Gong, X.; Liu, B.; Moses, D.; Bazan, G. C.; Heeger, A. J. *Adv. Mater.* **2005**, *17*, 274. (b) Bolink, H. J.; Brine, H.; Coronado, E.; Sessolo, M. *ACS Appl. Mater. Interfaces* **2010**, *2*, 2694. (c) Fang, J.; Wallikewitz, B. H.; Gao, F.; Tu, G.; Müller, C.; Pace, G.; Friend, R. H.; Huck, W. T. S. *J. Am. Chem. Soc.* **2010**, *133*, 683.

(10) Seo, J. H.; Namdas, E. B.; Gutacker, A.; Heeger, A. J.; Bazan, G. C. *Adv. Funct. Mater.* **2011**, *21*, 3667.

(11) (a) He, Z.; Zhang, C.; Xu, X.; Zhang, L.; Huang, L.; Chen, J.; Wu, H.; Cao, Y. *Adv. Mater.* **2011**, *23*, 3086. (b) Choi, H.; Park, J. S.; Jeong, E.; Kim, G.-H.; Lee, B. R.; Kim, S. O.; Song, M. H.; Woo, H. Y.; Kim, J. Y. *Adv. Mater.* **2011**, *23*, 2759. (c) He, Z.; Zhong, C.; Huang, X.; Wong, W.-Y.; Wu, H.; Chen, L.; Su, S.; Cao, Y. *Adv. Mater.* **2011**, *23*, 4636. (d) Seo, J. H.; Gutacker, A.; Sun, Y.; Wu, H.; Huang, F.; Cao, Y.; Scherf, U.; Heeger, A. J.; Bazan, G. C. *J. Am. Chem. Soc.* **2011**, *133*, 8416.

(12) (a) Mwaura, J. K.; Zhao, X.; Jiang, H.; Schanze, K. S.; Reynolds, J. R. *Chem. Mater.* **2006**, *18*, 6109. (b) Taranekar, P.; Qiao, Q.; Jiang, H.; Ghiviriga, I.; Schanze, K. S.; Reynolds, J. R. *J. Am. Chem. Soc.* **2007**, *129*, 8958. (c) Fang, Z.; Eshbaugh, A. A.; Schanze, K. S. *J. Am. Chem. Soc.* **2011**, *133*, 3063.

(13) Yang, R.; Garcia, A.; Korystov, D.; Mikhailovsky, A.; Bazan, G. C.; Nguyen, T.-Q. *J. Am. Chem. Soc.* **2006**, *128*, 16532.

(14) (a) Hodgkiss, J. M.; Tu, G.; Albert-Seifried, S.; Huck, W. T. S.; Friend, R. H. *J. Am. Chem. Soc.* **2009**, *131*, 8913. (b) Abrusci, A.; Santosh Kumar, R. S.; Al-Hashimi, M.; Heeney, M.; Petrozza, A.; Snaith, H. J. *Adv. Funct. Mater.* **2011**, *21*, 2571.

(15) Seo, J. H.; Jin, Y.; Brzezinski, J. Z.; Walker, B.; Nguyen, T.-Q. *ChemPhysChem* **2009**, *10*, 1023.

(16) Yang, R.; Wu, H.; Cao, Y.; Bazan, G. C. *J. Am. Chem. Soc.* **2006**, *128*, 14422.

(17) Zhu, Z.; Waller, D.; Gaudiana, R.; Morana, M.; Mühlbacher, D.; Scharber, M.; Brabec, C. *Macromolecules* **2007**, *40*, 1981.

(18) (a) Woo, H. Y.; Liu, B.; Kohler, B.; Korystov, D.; Mikhailovsky, A.; Bazan, G. C. *J. Am. Chem. Soc.* **2005**, *127*, 14721. (b) Ajayaghosh, A.; Chenthamarakshan, C. R.; Das, S.; George, M. V. *Chem. Mater.* **1997**, *9*, 644.

(19) (a) Nguyen, T.-Q.; Schwartz, B. J. *J. Chem. Phys.* **2002**, *116*, 8198. (b) Garcia, A.; Nguyen, T.-Q. *J. Phys. Chem. C* **2008**, *112*, 7054. (c) Davies, M. L.; Douglas, P.; Burrows, H. D.; da Graça Miguel, M.; Douglas, A. *J. Phys. Chem. B* **2011**, *115*, 6885.

(20) (a) Seo, J. H.; Nguyen, T.-Q. *J. Am. Chem. Soc.* **2008**, *130*, 10042. (b) Ishii, H.; Sugiyama, K.; Ito, E.; Seki, K. *Adv. Mater.* **1999**, *11*, 605.

(21) (a) Mühlbacher, D.; Scharber, M.; Morana, M.; Zhu, Z.; Waller, D.; Gaudiana, R.; Brabec, C. *Adv. Mater.* **2006**, *18*, 2884. (b) Lenes, M.; Morana, M.; Brabec, C. J.; Blom, P. W. M. *Adv. Funct. Mater.* **2009**, *19*, 1106.

(22) Sirringhaus, H.; Brown, P. J.; Friend, R. H.; Nielsen, M. M.; Bechgaard, K.; Langeveld-Voss, B. M. W.; Spiering, A. J. H.; Janssen, R. A. J.; Meijer, E. W.; Herwig, P.; de Leeuw, D. M. *Nature* **1999**, *401*, 685.

(23) He, Z.; Zhong, C.; Su, S.; Xu, M.; Wu, H.; Cao, Y. *Nat. Photon.* **2012**, *6*, 593.

(24) Cho, S.; Seo, J. H.; Kim, G.-H.; Kim, J. Y.; Woo, H. Y. *J. Mater. Chem.* **2012**, *22*, 21238.

(25) Hoven, C.; Yang, R.; Garcia, A.; Heeger, A. J.; Nguyen, T.-Q.; Bazan, G. C. *J. Am. Chem. Soc.* **2007**, *129*, 10976.